ELSEVIER

Journal of Power Sources 109 (2002) 427–430

JOURNAL OF POWER SOURCES

www.elsevier.com/locate/jpowsour

Synthesis and electrochemical characteristics of $LiCr_xNi_{0.5-x}Mn_{1.5}O_4$ spinel as 5 V cathode materials for lithium secondary batteries

Ki-Joo Hong, Yang-Kook Sun*

Department of Chemical Engineering, Hanyang University, Seoul 133-791, South Korea

Received 7 January 2002; accepted 25 February 2002

Abstract

A series of electrochemical spinel compounds, $LiCr_xNi_{0.5-x}Mn_{1.5}O_4$ ($x = 0$, 0.1, 0.3), are synthesized by a sol–gel method and their electrochemical properties are characterized in the voltage range of 3.5–5.2 V. Electrochemical data for $LiCr_xNi_{0.5-x}Mn_{1.5}O_4$ electrodes show two reversible plateaus at 4.9 and 4.7 V. The 4.9 V plateau is related to the oxidation of chromium while the 4.7 V plateau is ascribed to the oxidation of nickel. The $LiCr_{0.1}Ni_{0.4}Mn_{1.5}O_4$ electrode delivers a high initial capacity of 152 mAh g^{-1} with excellent cycleability. The excellent capacity retention of the $LiCr_{0.1}Ni_{0.4}Mn_{1.5}O_4$ electrode is largely attributed to structural stabilization which results from co-doping (chromium and nickel) and increased theoretical capacity due to substitution of chromium.

Keywords: Sol–gel method; Electrochemical characteristics; Lithium secondary batteries; Spinal; 5 V materials

1. Introduction

Lithium secondary batteries have been studied as power sources for portable electronic devices (cellular phones and laptop computers) and electric vehicles. Recently, spinel $LiMn_2O_4$ and its derivatives have generated great interest as promising cathode materials (positive electrodes) for lithium secondary batteries due to their low cost, abundance, and non-toxicity compared with layered oxides such as $LiCoO_2$ and $LiNiO_2$ [1–3]. Stoichiometric $LiMn_2O_4$, however, shows unacceptably large capacity fade on cycling due to Jahn–Teller distortion of trivalent Mn ions, and dissolution of Mn into the electrolyte [4–7]. The poor cycling behavior can be improved greatly by cation and anion substitution, and also surface passivation treatment of $LiMn_2O_4$ [8–11].

Recently, some research groups have reported that transition metal-substituted spinel materials ($LiM_xMn_{2-x}O_4$, M = Cr, Co, Fe, Ni, Cu) show a higher voltage plateau at around 5 V [12–15]. The capacity and voltage plateau in $Li/LiM_xMn_{2-x}O_4$ cells strongly depend on the type of transition metals (M) and their concentration. The high-voltage battery (5 V) system has an advantage of high specific energy. At such high voltage, however, the demand on the structural and chemical stability of the electrode as well as electrolyte becomes very severe. Although side reactions due to the electrolyte oxidation at the electrode surfaces can substantially deteriorate the cycling behavior of the electrode, improved electrolytes have recently made it possible to explore the potential range to about 5 V. The Ni-doped spinel electrode, $LiNi_xMn_{2-x}O_4$ delivers a capacity which is well below the theoretical capacity, while the Cr-doped electrode ($LiCr_xMn_{2-x}O_4$) rapidly loses its initial capacity during cycling [16–18].

In this paper, a study is made of the electrochemical properties of Ni- and Cr-doped $LiCr_xNi_{0.5-x}Mn_{1.5}O_4$ ($x = 0$, 0.1, 0.3) spinel electrodes in the 5 V region.

2. Experimental

$LiCr_xNi_{0.5-x}Mn_{1.5}O_4$ ($x = 0$, 0.1, 0.3) powders were prepared by a sol–gel method using glycolic acid as a chelating agent. $Li(CH_3COO)\cdot 2H_2O$, $Cr(NO_3)_3\cdot 9H_2O$, $Ni(CH_3COO)_2\cdot 4H_2O$, and $Mn(CH_3COO)_2\cdot 4H_2O$ (cationic ratio of Li:Cr:Ni:Mn = 1:x:0.5 − x:1.5, $x = 0$, 0.1 and 0.3) were dissolved in distilled water, and added dropwise to a continuously stirred aqueous solution of glycolic acid. The resultant solution was evaporated at 70–80 °C until a transparent sol and gel were obtained. The resulting gel precursors were decomposed at 450 °C for 5 h in air, and calcined at 900 °C in air for 15 h.

Powder X-ray diffraction (Rigaku, Rint-2000) using Cu Kα radiation was used to identify the crystalline phase of the

* Corresponding author.
E-mail address: yksun@hanyang.ac.kr (Y.-K. Sun).

0378-7753/02/$ – see front matter
PII: S0378-7753(02)00101-5

materials. The Li, Ni, and Mn contents in the resulting materials were determined by means of inductively coupled plasma-atomic emission spectrometry. The particle morphology of $LiCr_xNi_{0.5-x}Mn_{1.5}O_4$ powders was observed with a field emission scanning electron microscope (FE-SEM, Hitachi Co. S-4100).

Charge–discharge cycles were performed in CR2032 button type cells. The cell consisted of a cathode and a lithium metal anode separated by a porous polypropylene film. For the fabrication of the electrode, a mixture of 20 mg $LiCr_xNi_{0.5-x}Mn_{1.5}O_4$ powder and 12 mg conducting binder (8 mg TAB and 4 mg graphite) was pressed on to a 2.0 cm^2 stainless screen at 800 kg cm^{-2}. The electrolyte was a 1:2 mixture (v/v) of ethylene carbonate (EC) and dimethyl carbonate (DMC) containing 1 M The $LiPF_6$. The charge–discharge cycle was performed galvanostatically at a current density of 0.4 mA cm^{-2} between 5.2 and 3.5 V.

3. Results and discussion

Results of the chemical analysis of $LiCr_xNi_{0.5-x}Mn_{1.5}O_4$ ($x = 0$, 0.1 and 0.3) compounds obtained at 900 °C indicate almost stoichiometric contents. X-ray diffraction pattern (XRD) of $LiCr_xNi_{0.5-x}Mn_{1.5}O_4$ ($x = 0$, 0.1, 0.3) powders are given in Fig. 1. The Cr- and Ni-doped spinel, $LiCr_xNi_{0.5-x}Mn_{1.5}O_4$ ($x = 0.1$, 0.3) powders were each found to have a well-defined spinel structure without any impurity phases. On the other hand, XRD patterns for the Ni-doped spinel $LiNi_{0.5}Mn_{1.5}O_4$ powder (Fig. 1a) show small NiO peaks as an impurity as well as a spinel phase. This result is in agreement with previous work [12] that showed that low-crystalline, pure spinel $LiNi_{0.5}Mn_{1.5}O_4$ powders synthesized by a sol–gel method decomposed into mixture of NiO and spinel phase when calcined above 600 °C. Lee et al. [15] reported that the solubility limit of Ni in the $LiNi_xMn_{2-x}O_4$ system is 0.415.

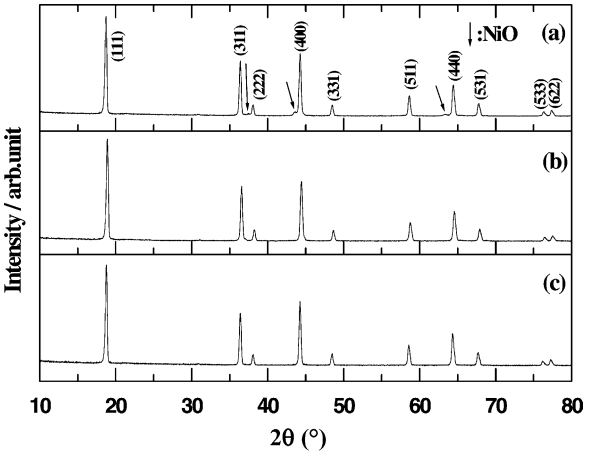

Fig. 1. X-ray diffraction patterns of $LiCr_xNi_{0.5-x}M_{1.5}O_4$ powders: (a)$x = 0$; (b) $x = 0.1$; (c) $x = 0.3$.

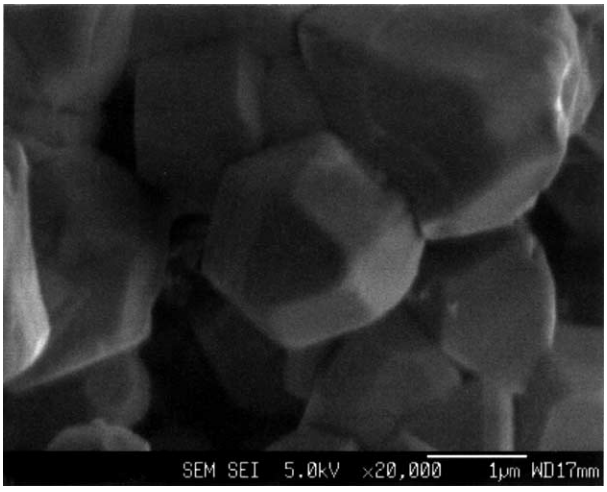

Fig. 2. Scanning electron micrograph of $LiCr_{0.1}Ni_{0.4}Mn_{1.5}O_4$ powders.

Scanning electron microscopy (SEM) images of the $LiCr_{0.1}Ni_{0.4}Mn_{1.5}O_4$ powders are shown in Fig. 2. The particles of the powders have well-developed (1 0 0) planes and a size distribution which ranges from 1 to 3 μm.

Charge–discharge curves for $LiCr_xNi_{0.5-x}Mn_{1.5}O_4$ ($x = 0$, 0.1, 0.3) e1ectrodes are presented in Fig. 3. The curves show a multiple number of distinct plateaus at different voltages. This indicates that the electrodes undergo multiple stages of reversible oxidation and reduction processes. Recent X-ray absorption fine structure (XAFS) analyses of electrochemically delithiated $LiM_xMn_{2-x}O_4$ (M = Cr, Co, and Ni) has shown [19] that the origin of the 5 V plateau is attributed to the oxidation of substituted M, while that of the 4 V plateau is oxidation of Mn^{3+} to Mn^{4+}. With two substituted cations, viz. Ni and Cr, for Mn, the charge–discharge curves for $LiCr_xNi_{0.5-x}Mn_{1.5}O_4$ ($x = 0.1$, 0.3) have two plateaus at 4.7 and 4.9 V, i.e. above 4.5 V. With increasing Cr in $LiCr_xNi_{0.5-x}Mn_{1.5}O_4$, the width of the 4.7 V plateau decreases while that of the 4.9 V plateau

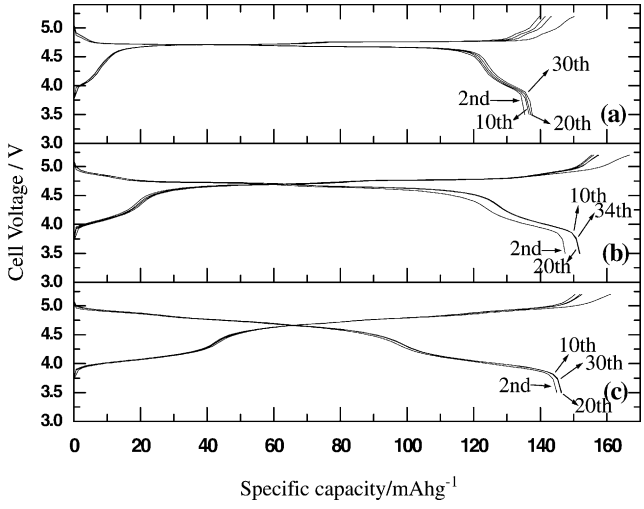

Fig. 3. Charge–discharge curves for $Li|LiCr_xNi_{0.5-x}Mn_{1.5}O_4$ cells in voltage range 3.5–5.2 V: (a) $x = 0$; (b) $x = 0.1$; (c) $x = 0.3$.

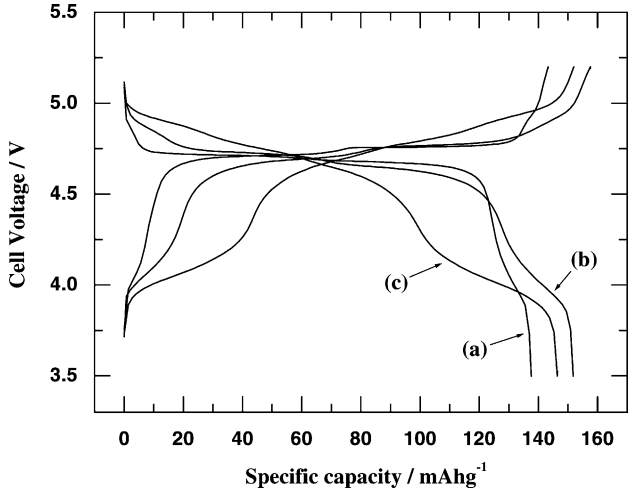

Fig. 4. Charge–discharge curves (10th cycle) for Li|$LiCr_xNi_{0.5-x}Mn_{1.5}O_4$ cells in voltage range 3.5–5.2 V: (a) $x = 0$; (b) $x = 0.1$; (c) $x = 0.3$.

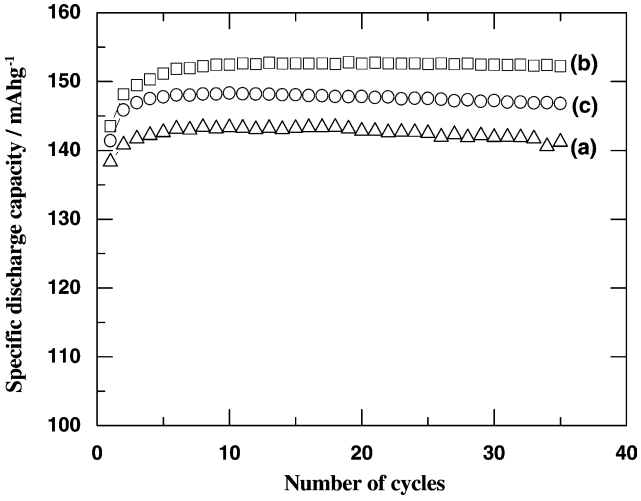

Fig. 6. Variation of specific discharge capacity as function of cycle number for Li|$LiCr_xNi_{0.5-x}Mn_{1.5}O_4$ cells: (a) $x = 0$; (b) $x = 0.1$; (c) $x = 0.3$.

increases. Shown in Fig. 4 are the voltage–capacity profiles for the 10th cycle. The Cr-free $LiNi_{0.5}Mn_{1.5}O_4$ electrode has a very flat discharge plateau at 4.7 V versus Li/Li^+. It is well known that the 4.7 V plateau is ascribed to the oxidation of Ni^{2+} to Ni^{4+} [15]. The 4.9 V plateau appears for the Cr- and Ni-doped $LiCr_xNi_{0.5-x}Mn_{1.5}O_4$ ($x = 0.1,\ 0.3$) electrode. With increasing Cr content, the capacity associated with the 4.7 V plateau decreases, while that resulting from the 4.9 V plateau increases. In order to obtain further supporting evidence of the Ni and Cr oxidation–reduction process, a plot of differential capacity versus voltage for the 10th cycle of the $LiCr_xNi_{0.5-x}Mn_{1.5}O_4$ ($x = 0$, 0.1, 0.3) is depicted in Fig. 5. Four oxidation and reduction peaks are observed in the voltage range of 3.5–5.2 V during cycling. With increasing Cr content, the peak intensity at 4.9 V becomes stronger. This indicates that the electrochemical process due to oxidation and reduction of Cr is responsible for the 4.9 V oxidation and reduction peaks.

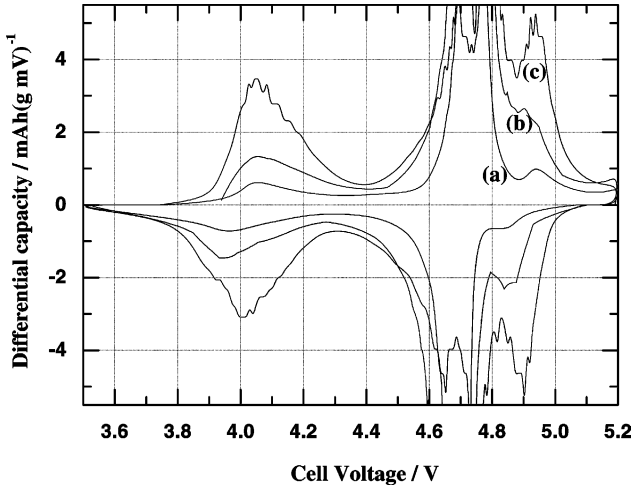

Fig. 5. Differential capacity vs. voltage for Li|$LiCr_xNi_{0.5-x}Mn_{1.5}O_4$ cells on 10th cycle: (a) $x = 0$; (b) $x = 0.1$; (c) $x = 0.3$.

The variation of discharge capacity as a function of cycle number for the $LiCr_xNi_{0.5-x}Mn_{1.5}O_4$ ($x = 0$, 0.1, 0.3) electrodes is given in Fig. 6. $LiCr_{0.1}Ni_{0.4}Mn_{1.5}O_4$ electrode delivers an initial discharge capacity of 152 mAh g^{-1} with excellent capacity retention, while the $LiNi_{0.5}Mn_{1.5}O_4$ electrode has a capacity of 137 mAh g^{-1}. As can be seen from Fig. 6, the discharge capacity falls to 146 mAh g^{-1} as Ni further replaces Cr to form $LiCr_{0.3}Ni_{0.2}Mn_{1.5}O_4$. All three electrodes maintain their initial discharge capacities after extended cycling. The improvement in discharge capacity following the partial replacement of Ni with Cr can be attributed largely to the stabilization of the spinel structure and an increase in theoretical capacity due to the low molecular weight of Cr compared with that of Ni. It is speculated that Cr doping removes impurity phases, such as the NiO shown in Fig. 1, and hence stabilizes the spinel structure. In addition, the strength of the Cr–O bond is another reason for the improved capacity retention of the Cr- and Ni-doped $LiCr_{0.1}Ni_{0.4}Mn_{1.5}O_4$ electrode because the bonding energy of Cr–O (427 kJ mol^{-1}) is stronger than that of Mn–O (402 kJ mol^{-1}) and Ni–O (391.6 kJ mol^{-1}) [20]. The stronger Cr–O bond can stabilize the spinel structure by assisting retention of the local symmetry during cycling. This prevents the structural disintegration of the material.

4. Conclusions

Excellent electrochemical and structural stability have been obtained for the 5 V cathode materials $LiCr_xNi_{0.5-x}Mn_{1.5}O_4$ ($x = 0$, 0.1, 0 3), which have cubic spinel structure and are prepared by a sol–gel method. The $LiCr_{0.1}Ni_{0.4}Mn_{1.5}O_4$ electrode delivers a very high initial discharge

capacity of 152 mAh g^{-1} with excellent cycleability compared with Ni-doped $LiNi_{0.5}Mn_{1.5}O_4$ electrode. The improved discharge capacity and capacity retention following the partial replacement of Ni with Cr can be attributed largely to stabilization of the spinel structure and an increase in theoretical capacity.

Acknowledgements

This work was supported in part by the Ministry of Information & Communication of Korea (''Support Project of University Information Technology Research Center'' supervised by KIPA).

References

[1] T. Ohzuka, M. Kitagawa, T. Hirai, J. Electrochem. Soc. 137 (1990) 769.
[2] D. Guyomard, J.-M. Tarascon, Solid State Ionics 69 (1994) 222.
[3] G.G. Amatucci, C.N. Schmutz, A. Bylr, C. Siala, A.S. Gozdz, D. Larcher, J.-M. Tarascon, J. Power Sources 69 (1997) 11.
[4] Y. Xia, Y. Zhou, M. Yoshio, J. Electrochem. Soc. 144 (1997) 2593.
[5] R.J. Gummow, A. de Kock, M.M. Thackeray, Solid State Ionics 69 (1994) 59.
[6] D.H. Jang, Y.J. Shin, S.M. Oh, J. Electrochem. Soc. 143 (1996) 2204.
[7] Y. Xia, Y. Zhou, M. Yoshio, J. Electrochem. Soc. 144 (1997) 2593.
[8] Y. Xia, N. Kumada, M. Yoshio, J. Power Sources 90 (2000) 135.
[9] J.-M. Tarascon, E. Wang, F.K. Shokoohi, W.R. Mckinnon, S. Colson, J. Electrochem. Soc. 138 (1995) 2859.
[10] L. Guohua, H. Ikuta, T. Uchida, M. Wakihara, J. Electrochem. Soc. 143 (1996) 178.
[11] C. Delmas, Mater. Sci. Eng. B3 (1989) 97.
[12] K. Amine, H. Tukamoto, H. Yasuda, Y. Fujita, J. Electrochem. Soc. 143 (1996) 1607.
[13] Q. Zhong, A. Bonakdarpour, M. Zhang, Y. Gao, J.R. Dahn, J. Electrochem. Soc. 144 (1997) 205.
[14] T. Ohzuku, S. Takeda, M. Iwanaga, J. Power Sources 81 (1999) 90.
[15] Y.S. Lee, Y.M. Todorov, T. Konishi, M. Yoshio, ITE Lett. 1 (2001) 1.
[16] C. Sigala, D. Guyomard, A. Verbaere, Y. Piffard, M. Tournoux, Solid State Ionics 81 (1995) 167.
[17] C. Sigala, A. Le Gal La Salle, Y. Piffard, D. Guyomard, J. Electrochem. Soc. A819 (2001) 148.
[18] C. Sigala, A. Le Gal La Salle, Y. Piffard, D. Guyomard, J. Electrochem. Soc. A826 (2001) 148.
[19] B. Ammundsen, D.J. Jones, J. Roziere, F. Villain, J. Phys. Chem. B 102 (1998) 7939.
[20] J.A. Dean, Lange's Handbook of Chemistry, 4th Edition, McGraw-Hill, New York, 1992, pp. 4.12–4.38.